



Special Feature: Organic Materials

Research Report

Electrical Properties of Polymethacrylate-grafted Carbon Nanotube Composites Prepared Using Surface-initiated Polymerization

Kenichi Hayashida

Report received on Dec. 17, 2012

■ABSTRACT■ Poly(cyclohexyl methacrylate)s (PCHMAs) were synthesized on carbon nanotubes (CNTs) using surface-initiated polymerization technique. Electrical properties of the PCHMA-grafted CNTs (PCHMA-CNTs) were systematically measured under direct current (DC) and alternating current (AC), and compared with those of conventional nanocomposites prepared by blending PCHMA with CNT (PCHMA/CNT). At a comparable volume fraction of CNT, PCHMA-CNT is 15 orders of magnitude higher DC volume resistivity than PCHMA/CNT. This excellent electrical insulation of PCHMA-CNT is achieved by the perfect isolation of individual CNTs owing to the high molecular weight PCHMAs densely grafted on the CNTs. The highly insulated PCHMA-CNT showed the same AC frequency dependence of impedance as neat PCHMA. This means PCHMA-CNT is a dielectric. The dielectric performance of PCHMA-CNT was evaluated by comparing with that of a barium titanate-filled PCHMA composite.

■KEYWORDS■ Multiwalled Carbon Nanotube, Surface-initiated Atom Transfer Radical Polymerization, Nanocomposite, Electrical Resistance, Impedance, Dielectric Properties

1. Introduction

Polymer/carbon nanotube (CNT) nanocomposite materials have been much developed over the past two decades.⁽¹⁻⁵⁾ CNTs impart good mechanical properties and high electrical and thermal conductivities to polymer materials at low CNT loading. Especially, only a few vol% of CNT loading can enhance electrical conductivity by several orders of magnitude, i.e., it turns insulator polymer materials to conductors.⁽⁶⁻¹⁰⁾ The conductive character is due to the formation of a three-dimensional conductive network of the CNT within the polymer matrix when the CNT content exceeds a critical value, known as a percolation threshold. The percolation thresholds are typically much less than 1 vol% for the polymer/CNT composites,⁽¹⁻⁵⁾ whereas more than 10 vol % of loading is required for conventional conductive fillers such as carbon black. The extremely low percolation threshold for the CNT means almost all polymer/CNT nanocomposites would become electrically conductive. The polymer/CNT nanocomposites, therefore, cannot be used for some applications demanding electrical insulation as well as good mechanical properties and/or high thermal conductivity (e.g. printed circuit boards, sealants for

semiconductor devices and light emitting diodes, insulators for the coils of motors). The unavoidable electrical conductivity of the polymer/CNT nanocomposites limits the extent of the applications.

A solution to prevent the electrical conductivity of polymer/CNT nanocomposites is that individual CNTs are completely covered with polymer matrix not to contact each other. Polymer grafting⁽¹¹⁻¹⁵⁾ on the surface of the CNT shows promise for insulation of the composite. Unlike physically adsorbed polymer chain, the covalently attached polymer chain would keep covering the CNT during processing such as compression molding at elevated temperature. In terms of the grafting polymer, not only its molecular weight but also its density is important for high electrical resistance. When the grafting density is low, even if the molecular weight is high, the CNT might approach each other within several nanometers, as indicated by previous morphological works.^(12,13) It is widely accepted that such small internanotube distance allows efficient electron tunneling between the CNTs (tunneling conduction).⁽¹⁶⁻¹⁹⁾ In contrast, a combination of a high molecular weight and a high grafting density makes it possible to isolate individual CNTs at a long distance by steric repulsion of “polymer brush”,⁽¹²⁻¹⁵⁾ and to produce a highly insulated polymer/CNT

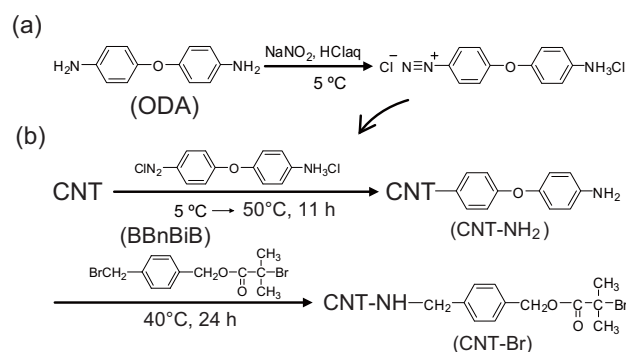
nanocomposite. We have recently developed a surface-initiated atom transfer radical polymerization (ATRP) method using an originally designed ATRP initiator, *p*-(bromomethyl)benzyl 2-bromoisobutylate (BBnBiB).⁽²⁰⁾ Our method has been modified to be applicable to multiwalled carbon nanotube (MWCNT), and the ATRP initiator moiety was covalently attached on the surface of the MWCNT. Using this ATRP initiator-modified MWCNT (CNT-Br), a series of poly(cyclohexyl methacrylate)s (PCHMAs) with various molecular weights densely grafted on MWCNT (PCHMA-CNTs) were synthesized.⁽²¹⁾ It was characteristic that all the polymer chains were tethered to the CNT in the PCHMA-CNT system, and the grafted polymer chains served as a matrix, implying that the CNT should be homogeneously dispersed in the polymer matrix. From many candidates of polymethacrylates, PCHMA was chosen for the grafted polymer because low polarity of the cyclohexyl group is expected to impart low water absorption to the polymethacrylate; high electrical resistance is susceptible to the water absorption. Another reason is that PCHMA has a comparatively high glass-transition temperature of 104°C, which is advantageous to high-temperature use.

In this report, we review electrical properties of PCHMA-CNT.^(21,22) The electrical resistance and the dielectric properties of PCHMA-CNT were systematically characterized under direct current (DC) and alternating current (AC), and compared to those of two conventional nanocomposites prepared by blending PCHMA with CNT or CNT-Br (PCHMA/CNT and PCHMA/CNT-Br). Furthermore, the performance of PCHMA-CNT as a dielectric material is evaluated by comparing with that of a barium titanate (BT)-filled PCHMA composite (PCHMA/BT).

2. Results and Discussion

ATRP-initiator modified MWCNT (CNT-Br) was synthesized as **Scheme 1**, where MWCNT with an average diameter of 10 nm was used. In the first step in Scheme 1(b), the CNT was amine-functionalized using an aryl diazonium salt method.^(23,24) We have found that a diazonium salt from 4,4'-oxydianiline (ODA) was stable at 5°C (Scheme 1(a)), and efficiently reacted with the CNT at the higher temperature. Thereby, the 4-(*p*-aminophenoxy)phenyl (APP) moiety of ODA was covalently attached to the CNT surface

(CNT-NH₂). We calculated the CNT weight fraction of CNT-NH₂, loading amounts of the APP moiety on the CNT and the element content of CNT-NH₂ using a weight increment of the CNT after the reaction (**Table 1**). The calculated values for CNT-NH₂ in Table 1 were supported by results of elemental analysis of H and N for CNT-NH₂. The experimental H and N contents in the parentheses in Table 1 are consistent with the calculated element contents from the sample weight. The APP moiety attached on the CNT was directly observed by transmission electron microscopy (TEM) (**Fig. 1(b)**). It is confirmed that an amorphous-like layer whose thickness is approximately 1.5 nm uniformly covers the CNT surface. In the second step in Scheme 1(b), CNT-NH₂ was reacted with BBnBiB,⁽²⁰⁾ and the ATRP-initiator moiety was introduced on the surface (CNT-Br). The Br content in CNT-Br was confirmed by combustion ion chromatography (Table 1). Finally, poly(cyclohexyl



Scheme 1 Preparation of ATRP initiator-modified CNT.

Table 1 Characteristics of the modified CNTs.

code	CNT weight fraction[a]	loading [mmol·g ⁻¹][b]	element content [wt %][c]		
			H	N	Br
CNT-NH ₂	0.693	2.4	1.7 (1.8)	2.3 (2.1)	-
CNT-Br	0.664	0.23	2.2 (1.9)	2.2 (2.0)	1.2 (1.1)

[a] Determined by the weight increment of the CNT sample after reaction. [b] The amount of the introduced moiety per unit weight of the CNT, which was calculated from the molecular weight of the moiety and the CNT weight fraction. [c] Estimated from the loading amounts. The value in the parentheses was obtained by elemental analysis of the modified CNTs.

methacrylate)-grafted CNT (CNT-PCHMA) was prepared by polymerization of the methacrylate monomer in the presence of CNT-Br. In the polymerization, free PCHMA was simultaneously prepared by an unfixed initiator, benzyl 2-bromoisobutylate (BnBiB), in order to confirm the molecular weight. The resultant free PCHMA was separated from CNT-PCHMA by centrifugation. The characterization result of the free PCHMA is shown in **Table 2** together with the calculated grafting density of the tethered PCHMA to the CNT. The grafting density was found to be $0.14 \text{ chains nm}^{-2}$, which is high

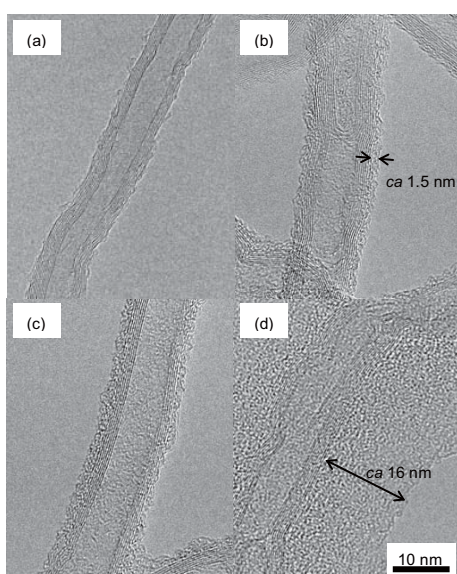


Fig. 1 TEM images of the modified CNTs. (a) CNT. (b) CNT-NH₂. (c) CNT-Br. (d) CNT-PCHMA.

Table 2 Characteristics of CNT-PCHMA.

CNT weight fraction[a]	$M_n \times 10^{-3}$ [b]	M_w/M_n [b]	loading [$\mu\text{mol} \cdot \text{g}^{-1}$][c]	grafting density [chains $\cdot \text{nm}^{-2}$][d]
0.155	93.8	1.33	53	0.14

[a] Determined by the weight increment of the CNT sample after polymer-grafting. [b] Values for the free polymer grown from an unfixed initiator. [c] The amount of the grafted polymer chains per unit weight of the CNT, which was calculated using the M_n and the CNT weight fraction. [d] Calculated from the loading amount of the polymer chains and the specific surface area of the CNT ($220 \text{ m}^2 \text{ g}^{-1}$).

enough to be regarded as “dense polymer brush”.⁽¹⁴⁾ The grafted PCHMA chain is clearly observed in the TEM image of CNT-PCHMA in Fig. 1(d).

For electrical measurements, a series of PCHMA-CNTs with various molecular weights from 60 k to 190 k were prepared as listed in **Table 3**. Note that the volume fraction of CNT, Φ_{CNT} decreases with increase in the molecular weight of PCHMA. For comparison, conventional nanocomposites (PCHMA/CNT and PCHMA/CNT-Br) were prepared by blending PCHMA ($M_n = 250 \text{ k}$, $M_w/M_n = 1.10$) with CNT or CNT-Br, which were designed to have the same Φ_{CNT} as PCHMA-CNT. A preliminary blending method using freeze-drying was applied in order to disperse the CNTs as homogeneously as possible.⁽¹⁵⁾ These nanocomposite samples were molded by compression of 10 MPa at 130°C prior to electrical measurements. The dispersion state of the CNT in the polymer matrix was observed by scanning electron microscopy (SEM). In this observation, the surfaces of the nanocomposites had been slightly etched with oxygen plasma in order to remove PCHMA. **Figures 2(a)-(c)** show high magnification SEM images of the nanocomposites with $\Phi_{\text{CNT}} = 0.055$. For PCHMA/CNT and PCHMA/CNT-Br, the CNTs are inhomogeneously dispersed in a submicron scale. This inhomogeneity is typical of polymer/CNT composites prepared by blending owing to the poor polymer/CNT compatibility. In contrast, the dispersivity of the CNT is surprisingly well for PCHMA-CNT. In the PCHMA-

Table 3 Characteristics of a series of PCHMA-CNTs

$M_n \times 10^{-3}$ [a]	fraction of CNT	
	weight [b]	volume[c]
60.2	0.214	0.143
72.5	0.188	0.124
82.5	0.171	0.112
102	0.145	0.094
143	0.111	0.071
190	0.087	0.055

[a] Estimated using the loading amount of the polymer chains on the CNT described in Table 2. [b] Determined by the weight increment of the CNT sample after polymer-grafting. [c] Calculated using a bulk density of 1.8 g cm^{-3} for the CNT and of 1.1 g cm^{-3} for the organic component.

CNT system, the CNT cannot agglomerate in the PCHMA matrix because all the PCHMA chains are tethered to the CNT. The excellent CNT dispersivity in PCHMA-CNT is also confirmed by the SEM image at low magnification (Fig. 2(f)). Polymer-grafting should be the best method of producing the perfectly homogeneous dispersion of CNT in a polymer matrix.

Figure 3 shows DC volume resistivity (ρ_{DC}) of the three types of nanocomposites. PCHMA/CNT has low ρ_{DC} less than 1 k Ω cm, which is a typical conductivity for nanocomposites containing CNTs. Because CNT is covered with the organic thin layer (~ 2 nm), PCHMA/CNT-Br has higher ρ_{DC} than PCHMA/CNT. However, PCHMA/CNT-Br has low ρ_{DC} of less than 10 G Ω cm, i.e., it becomes conductive when Φ_{CNT} is over 0.02, indicating that such thin layer on the CNT in PCHMA/CNT-Br easily allows the tunneling conduction. In contrast, PCHMA-CNT has very high ρ_{DC} of over 100 T Ω cm even at $\Phi_{CNT} = 0.094$, because the CNT is covered with the thick polymer shells in the PCHMA-CNT system. ρ_{DC} of PCHMA-CNT is 15 orders of magnitude higher than that of PCHMA/CNT at $\Phi_{CNT} = 0.055$. To our knowledge, such ultrahigh electrical resistance has not been reported for polymer/CNT nanocomposites. When Φ_{CNT} is over 0.1, ρ_{DC} of PCHMA-CNT is rapidly decreased in spite

of dense polymer grafting. This is because tunneling conduction dominantly occurs at high CNT concentration even in the PCHMA-CNT system as discussed in the references 21 and 22.

AC resistance, impedance Z , depends on the frequency f of an applied electric field. The magnitude of impedance $|Z|$ for the three types of nanocomposites is plotted as a function of f in the range of $10^2 - 10^6$ Hz in **Fig. 4**. PCHMA/CNT with $\Phi_{CNT} = 0.055$ shows very low $|Z|$, independent of f in all the frequency range. This is a typical conductor behavior. In the case of PCHMA-CNT with $\Phi_{CNT} = 0.055$ and 0.094, $|Z|$ is linearly increased with the decrease in f in the all frequency range similar to that of PCHMA. On the other hand, weak frequency dependence of $|Z|$ is observed for PCHMA-CNT with $\Phi_{CNT} = 0.14$ at below 10^4 Hz. Frequency dependence of PCHMA/CNT-Br shows intermediate behavior between those of PCHMA/CNT and PCHMA-CNT. PCHMA/CNT-Br has strong frequency dependence of $|Z|$ at $\Phi_{CNT} = 0.055$, while does almost no frequency dependence at $\Phi_{CNT} = 0.14$. Further characterization of these electrical behaviors was carried out by the introduction of the real and imaginary parts of Z . Because a material can be simply modeled as the electric circuit composed of a resistor and a capacitor connected in parallel, we

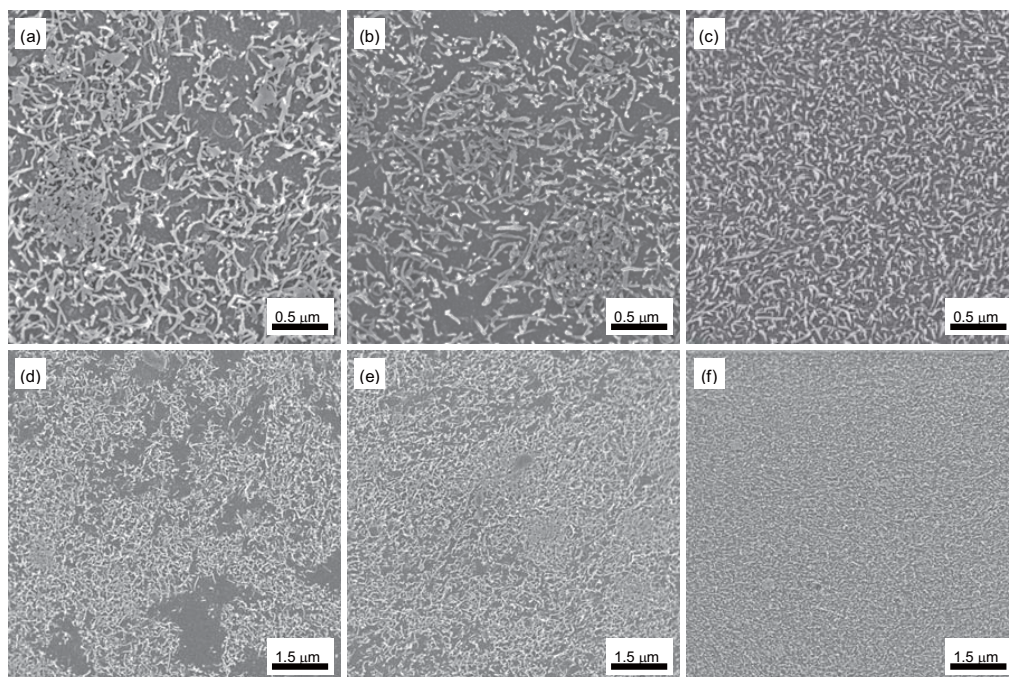


Fig. 2 High (upper) and low (lower) magnification SEM images of three types of nanocomposites with $\Phi_{CNT} = 0.055$: (a, d) PCHMA/CNT, (b, e) PCHMA/CNT-Br, (c, f) PCHMA-CNT.

can divide Z into the resistance R_p and the capacitive reactance X_{cp} as:

$$1/Z = 1/R_p + 1/(jX_{cp}); -X_{cp} = 1/(2\pi f C_p), \dots (1)$$

where j is the imaginary unit and C_p is the capacitance. The two components, R_p and $-X_{cp}$ for PCHMA/CNT-Br and PCHMA-CNT are shown in Fig. 5. Notice that X_{cp} has a minus sign. The corresponding spectra of

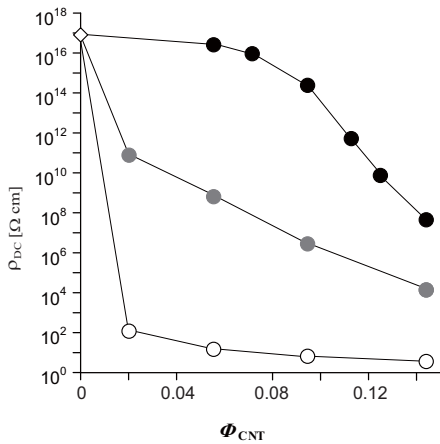


Fig. 3 DC volume resistivity (ρ_{DC}) of PCHMA (diamond) and three series of nanocomposites (circles) as a function of volume fraction of CNT. White circles, PCHMA/CNT; gray circles, PCHMA/CNT-Br; black circles, PCHMA-CNT.

PCHMA/CNT cannot be exhibited because the reactance component for PCHMA/CNT was too small to be measured precisely. For PCHMA-CNT with $\Phi_{CNT} = 0.094$, $-X_{cp}$ is much smaller than R_p in all the frequency range, which means almost all electric current is passed through the capacitor in the parallel resistor-capacitor (RC) circuit. That is, the PCHMA-CNT composite is a dielectric. In addition, $-X_{cp}$ of the

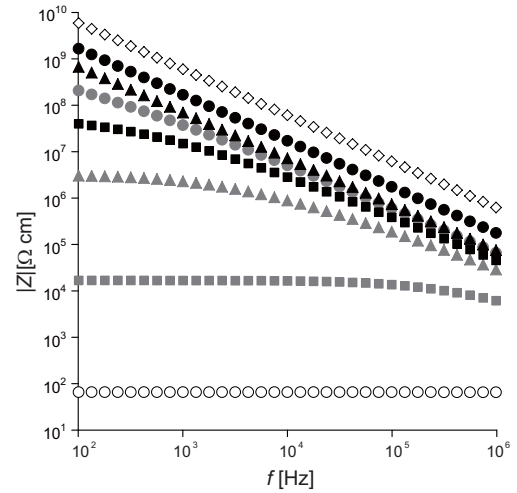


Fig. 4 Frequency f dependence of magnitude of impedance $|Z|$ of PCHMA (diamond) and three types of nanocomposites with $\Phi_{CNT} = 0.055$ (circles), $\Phi_{CNT} = 0.094$ (triangles), and $\Phi_{CNT} = 0.14$ (squares). White symbols, PCHMA/CNT; gray symbols, PCHMA/CNT-Br; black symbols, PCHMA-CNT.

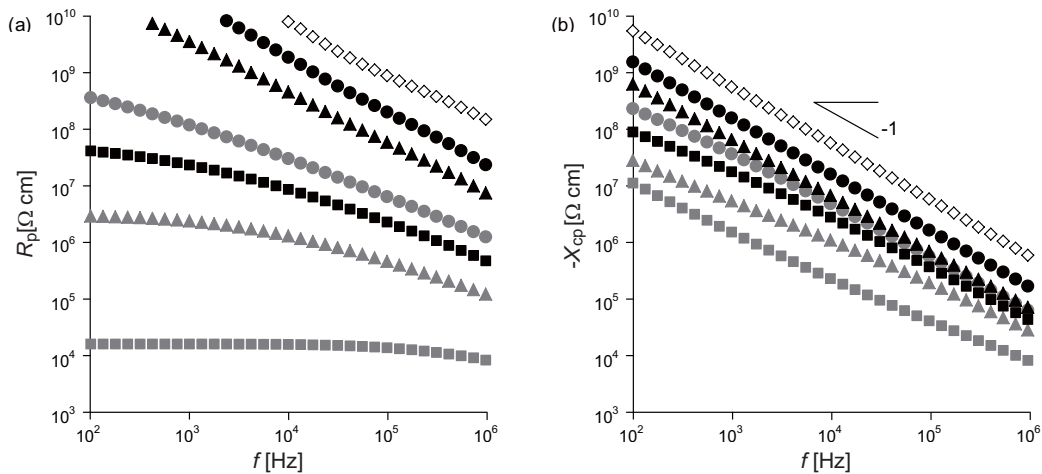


Fig. 5 f dependence of (a) resistance R_p and (b) capacitive reactance X_{cp} of PCHMA (diamond) and two types of nanocomposites with $\Phi_{CNT} = 0.055$ (circles), $\Phi_{CNT} = 0.094$ (triangles), and $\Phi_{CNT} = 0.14$ (squares). Gray symbols, PCHMA/CNT-Br; black symbols, PCHMA-CNT.

composite has a relationship described by $-X_{cp} \propto f^{-1}$ because C_p is almost constant. Similar dielectric behavior is also observed for PCHMA and PCHMA-CNT with $\Phi_{CNT} = 0.055$. Unlike these PCHMA-CNT composites, PCHMA-CNT with $\Phi_{CNT} = 0.14$ has a transition from a dielectric ($R_p > -X_{cp}$) to a conductor ($R_p < -X_{cp}$) at $\sim 10^3$ Hz. This is because R_p at $\Phi_{CNT} = 0.14$ is small especially at the low frequencies owing to the tunneling conduction.

Figure 6 shows frequency dependence of dielectric constant, ϵ_r' and dielectric loss factor, ϵ_r'' of PCHMA/CNT-Br and PCHMA-CNT in the wide range of $10^{-2} - 10^8$ Hz. For PCHMA/CNT-Br, ϵ_r' and ϵ_r'' are significantly increased with the decrease in f . In many previous studies on polymer/CNT nanocomposites, the giant ϵ_r' at low frequencies has been attributed to space charge polarization and/or interface polarization between the CNT and the polymer matrix.⁽²⁵⁻²⁹⁾ Therefore, it has also been suggested that the interaction at the polymer/CNT interface and the dispersivity of the CNT in the polymer matrix are

important for the enhancement in ϵ_r' .^(25,28,29) However, the discrepant phenomena have been found for our PCHMA-CNT system. ϵ_r' of PCHMA-CNT with $\Phi_{CNT} = 0.055$ is almost independent of f even at the low frequency although the dispersivity of the CNT is surprisingly good (Fig. 2(c)). Furthermore, the polymer/CNT interface should be strong because of polymer-grafting on the CNT. On the other hand, PCHMA-CNT with $\Phi_{CNT} = 0.14$ where the tunneling conduction is observed, exhibits the giant ϵ_r' at the low frequencies as previously reported. This fact means that the increase in ϵ_r' should not result from the interface polarization and/or the space charge polarization. At present, it is speculated that the locally amplified electric field by the tunneling conduction brings the giant ϵ_r' at the low frequencies in the polymer/CNT composite systems. This explanation is consistent with no increase in ϵ_r' at the low frequencies for PCHMA-CNT with $\Phi_{CNT} = 0.055$.

For the PCHMA/CNT-Br system, R_p is usually much smaller than $-X_{cp}$, suggesting that the microcapacitor

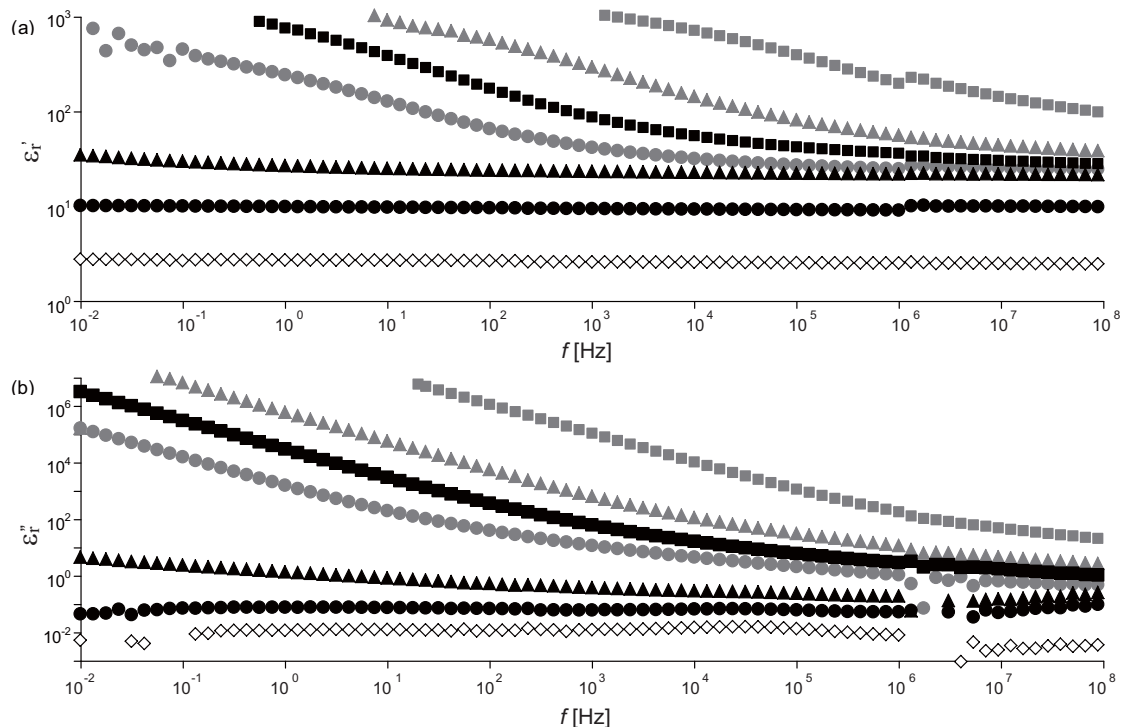


Fig. 6 f dependence of (a) dielectric constant ϵ_r' and (b) dielectric loss factor ϵ_r'' of PCHMA (diamond) and two types of nanocomposites with $\Phi_{CNT} = 0.055$ (circles), $\Phi_{CNT} = 0.094$ (triangles), and $\Phi_{CNT} = 0.14$ (squares). Gray symbols, PCHMA/CNT-Br; black symbols, PCHMA-CNT.

is a resistor rather than a capacitor, i.e., it is a conductor. In contrast, PCHMA-CNTs with $\Phi_{\text{CNT}} = 0.055$ and 0.094 have very low ϵ_r'' in all the frequency range (Fig. 6(b)). This is because the internanotube distance is large enough to prevent the tunneling conduction. ϵ_r' and the dissipation factor ($\tan\delta = \epsilon_r''/\epsilon_r'$) of PCHMA/CNT-Br and PCHMA-CNT at 1 MHz are plotted in Fig. 7. For PCHMA-CNT, $\tan\delta$ is below 0.01, when Φ_{CNT} is less than 0.1. For example, ϵ_r' of 22.5 and $\tan\delta$ of 0.010 are obtained at $\Phi_{\text{CNT}} = 0.094$. This $\tan\delta$ value is much lower than those for polymer/CNT composites that have been reported.⁽¹⁹⁻²³⁾ The dielectric property of the low loss PCHMA-CNT is compared to that of PCHMA filled with barium titanate (PCHMA/BT). In Fig. 8(a), the plots of $\log \epsilon_r'$ versus Φ_{CNT} and Φ_{BT} show linear relationships for both the composites. The slope of the relationship for PCHMA-CNT is five times larger than those for PCHMA/BT, implying the CNT is more effective than the BT for enhancement in ϵ_r' of polymer materials. This finding is a major advantage of PCHMA-CNT over PCHMA/BT for polymer material design. For example, about ten times enhancement in ϵ_r' can be achieved with only 10 vol% of the CNT for PCHMA-CNT. In addition, $\tan\delta$ of PCHMA-CNT is as low as that of PCHMA/BT (Fig. 8(b)), and PCHMA-CNT has smaller frequency dependence of the dielectric properties than PCHMA/BT (Fig. 8(c)).

3. Conclusion

In summary, we synthesized a series of MWCNTs on which poly(cyclohexyl methacrylate)s (PCHMAs) with various molecular weights were densely grafted (PCHMA-CNTs), using a modified SI-ATRP

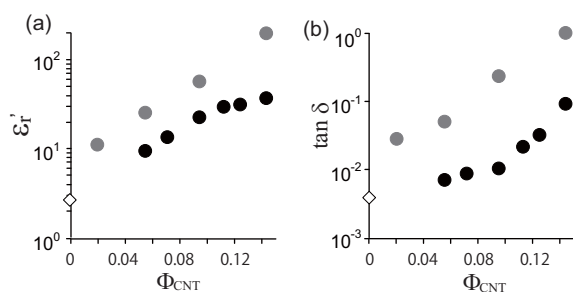


Fig. 7 (a) ϵ_r' and (b) dissipation factor ($\tan\delta$) of PCHMA (diamond) and two types of nanocomposites (circles) at 1 MHz as a function of Φ_{CNT} . Gray circles, PCHMA/CNT-Br; black circles, PCHMA-CNT.

technique. PCHMA-CNT was found to have high grafting density of 0.14 chains nm^{-2} , which is enough to be referred to as “dense polymer brush”. PCHMA-CNT has ultrahigh electrical resistance when M_n of the grafted PCHMA exceeds 100 k ($\Phi_{\text{CNT}} < 0.1$); At $\Phi_{\text{CNT}} = 0.055$, DC volume resistivity of PCHMA-CNT is 15 orders of magnitude higher than that of a conventional nanocomposite (PCHMA/CNT). This is because the polymer brush with a combination of the high molecular weight and the high grafting density isolates individual CNTs at a long distance in the PCHMA-CNT system. In addition, impedance analysis reveals the highly insulated PCHMA-CNT has the same electrical nature as neat PCHMA, i.e., it is a dielectric. Furthermore, we have demonstrated that the CNT is five times more effective than the BT for the enhancement in ϵ_r' of polymer materials.

4. Experimental

Preparation: MWCNT with an average diameter and length of 10 nm and 1.5 μm , respectively, was obtained from Nanocyl SA. A series of PCHMA-grafted MWCNTs (PCHMA-CNT) were synthesized as

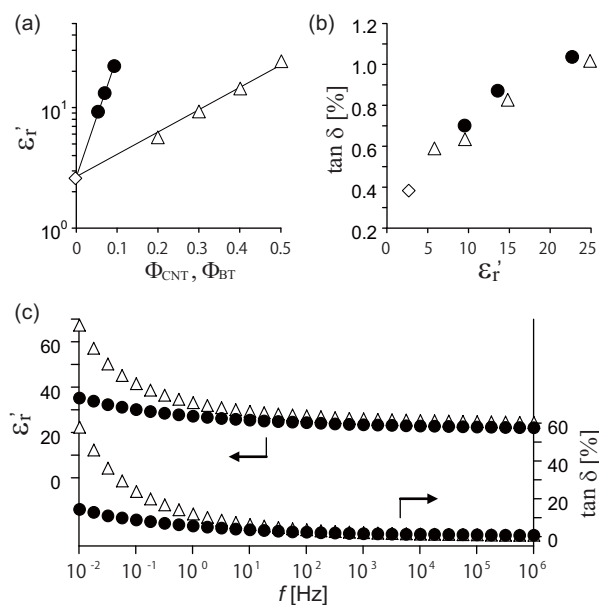


Fig. 8 Comparison of dielectric properties between PCHMA-CNT (black circle) and PCHMA/BT (white triangle). (a) ϵ_r' as a function of Φ_{CNT} and Φ_{BT} , and (b) ϵ_r' - $\tan\delta$ plot at 1 MHz. The values for PCHMA are plotted with a diamond symbol. (c) f dependence of ϵ_r' and $\tan\delta$ of PCHMA-CNT with $\Phi_{\text{CNT}} = 0.094$ and PCHMA/BT with $\Phi_{\text{BT}} = 0.50$.

reported previously.⁽²¹⁾ Conventional nanocomposites (PCHMA/CNT, PCHMA/CNT-Br and PCHMA/BT) were prepared by blending PCHMA with CNT, CNT-Br, or BT, where BT particle with an average size of less than 100 nm (Aldrich) was used.⁽²²⁾ These nanocomposite samples were molded into 15 mm square specimens with a thickness of ~0.9 mm by compression of 10 MPa at 130°C. For impedance measurements in the frequency range of 10^{-2} – 10^6 Hz, two gold electrodes 11 mm square were deposited on the top and bottom of the specimen at a distance of 2 mm from the edge of the specimen.

Measurements: The modified CNTs were observed using a transmission electron microscope (JEOL, JEM-2100F) operated at an accelerating voltage of 200 kV. The specimens of the nanocomposites were observed using a scanning electron microscope (Hitachi, S4300) operated at an accelerating voltage of 2 kV. For impedance measurement, three types of impedance analyzers, Solartron 126096W, Agilent E4980A, and Agilent E4991A, were used depending on the frequency range, 10^{-2} – 10^2 Hz, 10^2 – 10^6 Hz, and 10^6 – 10^8 Hz, respectively.

Acknowledgements

TEM and SEM observations were carried out by Mr. Noritomo Suzuki and Ms. Yoriko Matsuoka at Toyota Central R&D Labs. Inc., respectively.

References

- (1) Coleman, J. N., Khan, U. and Gun'ko, Y. K., *Adv. Mater.*, Vol. 18, No. 6 (2006), pp. 689-706.
- (2) Moniruzzaman, M. and Winey, K. I., *Macromolecules*, Vol. 39, No. 16 (2006), pp. 5194-5205.
- (3) Bauhofer, W. and Kovacs, J. Z., *Comp. Sci. Technol.*, Vol. 69, No. 10 (2009), pp. 1486-1498.
- (4) Spitalsky, Z., Tasis, D., Paragelis, K. and Costas, G., *Prog. Polym. Sci.*, Vol. 35, No. 3 (2010), pp. 357-401.
- (5) Byrne, M. T. and Gun'ko, Y. K., *Adv. Mater.*, Vol. 22, No. 15 (2010), pp. 1672-1688.
- (6) Sandler, J., Shaffer, M. S. P., Prasse, T., Bauhofer, W., Schulte, K. and Windle, A. H., *Polymer*, Vol. 40, No. 21 (1999), pp. 5967-5971.
- (7) Du, F., Scogna, R. C., Zhou, W., Brand, S., Fischer, J. E. and Winey, K. I., *Macromolecules*, Vol. 37, No. 24 (2004), pp. 9048-9055.
- (8) Li, J., Ma, P. C., Chow, W. S., To, C. K., Tang, B. Z. and Kim, J.-K., *Adv. Funct. Mater.*, Vol. 17, No. 16 (2007), pp. 3207-3215.
- (9) Deng, H., Skipa, T., Bilotti, E., Zhang, R., Lellinger, D., Mezzo, L., Fu, Q., Alig, I. and Peijs, T., *Adv. Funct. Mater.*, Vol. 20, No. 9 (2010), pp. 1424-1432.
- (10) Huang, Y. Y. and Terentjev, E. M., *Adv. Funct. Mater.*, Vol. 20, No. 23 (2010), pp. 4062-4068.
- (11) Homenick, C. M., Lawson, G. and Adronov, A., *Polym. Rev.*, Vol. 47, No. 2 (2007), pp. 265-290.
- (12) Yezek, L., Schartl, W., Chen, Y., Gohr, Y. K. and Schmidt, M., *Macromolecules*, Vol. 36, No. 11 (2003), pp. 4226-4234.
- (13) Akcora, P., Liu, H., Kumar, S. K., Moll, J., Li, Y., Benicewicz, B. C., Schadler, L. S., Acehan, D., Panagiotopoulos, A. Z., Pryamitsyn, V., Ganesan, V., Ilavsky, J., Thiyagarajan, P., Colby, R. H. and Douglas, J. F., *Nat. Mater.*, Vol. 8, No. 4 (2009), pp. 354-359.
- (14) Tsujii, Y., Ohno, K., Yamamoto, S., Goto, A. and Fukuda, T., *Adv. Polym. Sci.*, Vol. 197, (2006), pp. 1-45.
- (15) Hayashida, K., Tanaka, H. and Watanabe, O., *Polym. Int.*, Vol. 60, No. 8 (2011), pp. 1194-1200.
- (16) Connor, M. T., Roy, S., Ezquerro, T. A. and Balta Calleja, F. J., *Phys. Rev. B*, Vol. 57, No. 4 (1998), pp. 2286-2294.
- (17) Kilbride, B. E., Coleman, J. N., Fraysse, J., Fournet, P., Cadek, M., Drury, A., Hutzler, S., Roth, S. and Blau, W. J., *J. Appl. Phys.*, Vol. 92, No. 7 (2002), pp. 4024-4030.
- (18) Li, H.-C., Lu, S.-Y., Syue, S.-H., Hsu, W.-K. and Chang, S.-C., *Appl. Phys. Lett.*, Vol. 93, No. 3 (2008), 033104.
- (19) Fritzsche, J., Lorenz, H. and Kluppel, M., *Macromol. Mater. Eng.*, Vol. 294, No. 9 (2009), pp. 551-560.
- (20) Hayashida, K., Tanaka, H. and Watanabe, O., *Polymer*, Vol. 50, No. 26 (2009), pp. 6228-6234.
- (21) Hayashida, K. and Tanaka, H., *Adv. Funct. Mater.*, Vol. 22, No. 11 (2012), pp. 2338-2344.
- (22) Hayashida, K., *RSC Adv.*, Vol. 3, No. 1 (2013), pp. 221-227.
- (23) Bahr, J. L. and Tour, J. M., *Chem. Mater.*, Vol. 13, No. 11 (2001), pp. 3823-3824.
- (24) Christopher, A. D. and Tour, J. M., *Nano Lett.*, Vol. 3, No. 9 (2003), pp. 1215-1218.
- (25) Dang, Z.-M., Wang, L., Yin, Y., Zhang, Q. and Lei, Q.-Q., *Adv. Mater.*, Vol. 19, No. 6 (2007), pp. 852-857.
- (26) Zhang, J., Mine, M., Zhu, D. and Matsuo, M., *Carbon*, Vol. 47, No. 5 (2009), pp. 1311-1320.
- (27) Dang, Z.-M., Yao, S.-H., Yuan, J.-K. and Bai, J., *J. Phys. Chem. C*, Vol. 114, No. 31 (2010), pp. 13204-13209.
- (28) Yuan, J.-K., Yao, S.-H., Dang, Z.-M., Sylvestre, A., Genestorux, M. and Bai, J., *J. Phys. Chem. C*, Vol. 115, No. 13 (2006), pp. 5515-5521.
- (29) Liu, H., Shen, Y., Song, Y., Nan, C.-W., Lin, Y. and Yang, X., *Adv. Mater.*, Vol. 23, No. 43 (2011), pp. 5104-5108.

Scheme 1 and Fig. 1

Reprinted from *Advanced Functional Materials*, Vol. 22

(2012), pp.2338-2344, Hayashida, K., Tanaka, H.,
Ultrahigh Electrical Resistance of Poly(cyclohexyl
methacrylate)/Carbon Nanotube Composites Prepared
Using Surface-initiated Polymerization, © 2012 John
Wiley & Sons, Inc, with permission from John Wiley &
Sons, Inc.

Figs. 4-8

Reprinted from RSC Adv., Vol. 3, No. 1 (2013),
pp. 221-227, Hayashida, K., Dielectric Properties of
Polymethacrylate-grafted Carbon Nanotube Composites,
© 2013 The Royal Society of Chemistry, with permission
from the Royal Society of Chemistry.

Kenichi Hayashida

Research Field:

- Synthesis and Properties of Polymer
Nanocomposite Materials

Academic Degree: Dr.Eng.

Academic Society:

- The Society of Polymer Science, Japan

Award:

- Inoue Research Aid for Young Scientists, 2008

